Phytotaxa 782 (3): 239–253
https://www.mapress.com/pt/
Copyright © 2026 Magnolia Press

Article

ISSN 1179-3155 (print edition)
PHYTOTAXA
ISSN 1179-3163 (online edition)

https://doi.org/10.11646/phytotaxa.782.3.3

Epitypification of *Mesotaenium endlicherianum* and the description of two new *Mesotaenium* species

ANNA BUSCH[1*], KARL-HEINZ LINNE VON BERG[2], TATYANA DARIENKO[3] & SEBASTIAN HESS[4]
[1]*Department of Biology, Technical University Darmstadt, Schnittspahnstraße 3, D-64287 Darmstadt, Germany*
busch@bio.tu-darmstadt.de; https://orcid.org/0000-0002-5377-7150
[2]*Auf dem Buechel 54, D-53925, Kall, Germany*
linnevonberg@uni-koeln.de; https://orcid.org/0009-0000-5417-4936
[3]*Department of Applied Bioinformatics, Institute for Microbiology and Genetics, Georg-August-University Göttingen, Julia-Lermontowa-Weg 3, D-37077 Göttingen, Germany*
tdarien@gwdg.de; https://orcid.org/0000-0002-1957-0076
[4]*Department of Biology, Technical University Darmstadt, Schnittspahnstraße 3, D-64287 Darmstadt, Germany*
hesslab@bio.tu-darmstadt.de; https://orcid.org/0000-0003-1262-8201
[*]*Author for correspondence*

Abstract

Since the emergence of molecular phylogenetics, several genera within the Zygnematophyceae have been shown to be polyphyletic. Polyphyly is particularly apparent among taxa with a plain morphology such as the genus *Mesotaenium* Nägeli. Currently, this genus name is applied to zygnematophyte species of several distinct evolutionary lineages, which require a taxonomic revision. For this, the type species, *M. endlicherianum* Nägeli, needs to be clearly assigned to one of these lineages. We studied three closely related *Mesotaenium*-like strains of lineage Meso-2 with an integrative approach combining morphology, cell cycle characterisation, and molecular phylogenetics based on the *rbcL* gene. Our results reveal clear genetic and morphological differences among the strains, supporting their recognition as three distinct species. To establish a stable taxonomic framework, we epitypify *M. endlicherianum* based on strain SAG 12.97 and thus formally assign the genus *Mesotaenium* to lineage Meso-2. Additionally, we describe two new species for this clade and establish the common cellular details of the latter. The defined phylogenetic placement of *Mesotaenium* established in this work now paves the way for additional taxonomic revisions of provisionally described lineages.

Key words: Zygnematophyceae, Serritaeniales, *Mesotaenium endlicherianum*, Integrative Taxonomy

Introduction

The Zygnematophyceae comprise species with diverse morphologies, including single-celled desmids and several lineages with unbranched filaments (Hall & McCourt 2016; Hess *et al.* 2022). Currently, there are approximately 170 described genera and 4,000 described species (Guiry & Guiry 2026). However, phylogenetic studies have indicated that many genera are polyphyletic, including *Micrasterias* C. Agardh ex Ralfs (1848: 68), *Euastrum* Ehrenberg ex Ralfs (1848: 78), *Cosmarium* Corda ex Ralfs (1848: 91), *Actinotaenium* (Nägeli) Teiling (1954: 385), *Cylindrocystis* Meneghini ex De Bary (1858: 35, 74), and *Mesotaenium* Nägeli (1849: 108) (Ralfs 1848; Nägeli 1849; de Bary 1858; Teiling 1954). Furthermore, a large proportion of described species still lack molecular data, leaving the phylogenetic placement of these taxa unresolved (Gontcharov 2008; Hall *et al.* 2008; Gontcharov & Melkonian 2010; Busch & Hess 2022a; De Araújo *et al.* 2022). Historically, many zygnematophyte species have mainly been described based on morphological traits, such as cell shape and size of vegetative material (Nägeli 1849; Hansgirg 1886; West & West 1904). The use of limited morphological traits in original descriptions and the variability of such traits in nature has resulted in taxonomic uncertainties and a convoluted taxonomic history with numerous infraspecific taxa and synonyms (Guiry & Guiry 2026). The genus *Mesotaenium* is particularly challenging, as its members exhibit a relatively plain morphology: They represent more or less cylindrical unicells with smooth cell walls and ribbon-like chloroplasts. Recent sampling efforts combined with molecular phylogenetic analyses revealed that *Mesotaenium*-like zygnematophytes are more diverse than previously recognised, representing 12 distinct evolutionary lineages within

Accepted by Dmitry Kapustin: 13 Oct. 2026; published: 30 Oct. 2026

Licensed under Creative Commons Attribution-N.C. 4.0 International https://creativecommons.org/licenses/by-nc/4.0/

the Zygnematophyceae (Busch & Hess 2022a). Two lineages have already been assigned to other genera (*Ancylonema* Berggren (1872: 865) and *Serritaenia* A. Busch & S. Hess (2022: 114) (Berggren 1871; Busch & Hess 2022b)) while the remaining lineages still have a provisional naming (Meso-1 to Meso-10) (Procházková *et al.* 2021; Busch & Hess 2022a, b). For future taxonomic revisions of these lineages, it is essential to clarify which of them should be assigned to the genus *Mesotaenium*. In this context, pinpointing the type species, *M. endlicherianum* Nägeli (1849: 108) (Nägeli 1849), is of particular importance.

Mesotaenium endlicherianum was first described by Nägeli in 1849, with Zurich, Switzerland designated as its type locality (Nägeli 1849). Since then, five varieties of this species have been described on the basis of slight morphological differences in cell size and chloroplast shape (for details, see Buech 1967). Two of these taxa were later established as separate species (change in rank), namely *M. caldariorum* (Lagerheim) Hansgirg (Hansgirg 1886; Lagerheim 1886) and *M. minimum* J.A. Cushman (Cushman 1906). In the 1990s, one algal strain (SAG 12.97) was isolated from a lake in Portugal and referred to as *M. endlicherianum* (Luo & Hall 2007; Hall *et al.* 2008; Civáň *et al.* 2014; Matasci *et al.* 2014; Cheng *et al.* 2019). However, some authors mentioned minor morphological differences between the strain SAG 12.97 and the original description of *M. endlicherianum* (Gontcharov *et al.* 2003, 2004; Busch & Hess 2022a). Since the genome of strain SAG 12.97 was published (Cheng *et al.* 2019), strain SAG 12.97 has been featured in around 30 studies under the name *M. endlicherianum* (Dadras *et al.* 2023b; Rieseberg *et al.* 2023, 2025) and became widely recognised in fields outside phycology as well, e.g., molecular plant sciences (de Roij *et al.* 2025; Fujimoto *et al.* 2025; Marks & Petersen 2026). However, due to the mentioned morphological differences (Gontcharov *et al.* 2003, 2004; Busch & Hess 2022a) the correct taxonomic assignment of strain SAG 12.97 is still to be worked out. To clarify or define the species identity of this extensively studied zygnematophyte, a detailed morphological evaluation and a taxonomic assessment is required.

In this study, we assess the taxonomy of strain SAG 12.97, as well as that of two closely related strains, ACOI 2703 and SAG 2677. We report the morphology of axenic cultures grown under controlled conditions, compare morphological data with original species descriptions, and resolve the relationships of the studied strains with *rbcL* gene sequence data. Considering the mentioned history of strain SAG 12.97, we designate an epitype for *M. endlicherianum* based on this strain and unambiguously link the type species of *Mesotaenium* to a defined phylogenetic lineage. Furthermore, two new *Mesotaenium* species, *M. nodulatum* and *M. crassum*, are described, extending our knowledge on species diversity in this increasingly recognised zygnematophyte lineage.

Materials and Methods

Sampling, isolation and maintenance of algae

Strains were either ordered from culture collections or isolated from natural samples during this study (Table 1). Bacteria-free cultures of all strains (SAG 12.97, ACOI 2703, SAG 2677) were established by the spray plating method (Busch & Hess 2022b). The algae were cultured in Waris-H medium (McFadden & Melkonian 1986) at 15°C under an irradiance of 30–50 µmol photons m^{-2} s^{-1}, with a 14:10 h light-dark cycle. Algal strains are available through the Culture Collection of Algae at University Goettingen (SAG, Göttingen, Germany) and the Coimbra Collection of Algae (ACOI, Coimbra, Portugal).

TABLE 1. Studied strains and associated information.

Strain	Species	Origin	Collector
SAG 12.97 (ACOI 451)	*M. endlicherianum*	Portugal, Quiaios, Lagoa das Braças, plankton, 1991	O. Lourenço
ACOI 2703	*M. crassum*	Spain, between Ceada and Miranda do Douro, brook, 2006	L. Santos
SAG 2677 (N74 author's collection)	*M. nodulatum*	Germany, Gemünd-Malsbenden, forest trail, 2020	K.H. Linne von Berg

Light microscopy

Regular observations of cultures were done with the Motic AE2000 inverted microscope (Motic, Hong Kong) equipped with a MikroLive 6.4MP CMOS camera (MikroLive, Oppenau, Germany). For high-resolution imaging, the Zeiss IM35 inverted microscope and the Zeiss Axio Observer inverted microscope (Carl Zeiss, Oberkochen, Germany) both equipped with high-NA oil immersion objectives and differential interference contrast optics were used. Colour balance and contrast of light micrographs were adjusted with Photoshop CS4 (Adobe Inc., California, USA). Extracellular mucilage was visualised with Indian ink. Time-lapse microscopy was done with the Zeiss Axio Observer inverted microscope equipped with the objective lens Plan-Neofluar 40×/1.3 and the Axiocam 512 colour (Carl Zeiss, Oberkochen). For confocal laser scanning microscopy, algal cells were collected by centrifugation (500 *g*, 5 min), mixed with Calcofluor White solution (0.1% in H_2O), and imaged with the Leica TSC SP8 setup (Leica, Wetzlar, Germany). The plastid morphology was visualised using chlorophyll autofluorescence (excitation: 445 nm; emission: 650–700 nm) and the algal cell wall by cellulose-bound Calcofluor White fluorescence (excitation: 405 nm; emission: 410–500 nm). Z-stacks were recorded with a step size of 0.42 µm and processed with the Leica LAS AF software (Leica, Wetzlar, Germany) and the image processing package Fiji (https://fiji.sc/, (Schindelin *et al.* 2012)).

DNA sequencing, alignment and molecular phylogenetics

About 15 ml of an algal culture were harvested by centrifugation (1,000 *g*, 10 min), transferred to 2 ml tubes, washed with nuclease free water and centrifuged (10,000 *g*, 2 min). Supernatant was removed, 20 Yttrium-stabilised zirconia ceramic balls (SiLibeads Typ ZY 6.0, 2,8–3,2 mm, Sigmund Lindner, Warmensteinach, Germany) were added, samples were frozen at − 80°C and freeze dried with the Alpha 2-4 LD plus freeze-dryer (Christ, Osterode, Germany). Freeze dried cells were lysed by shaking (30 Hertz, 2 min, two times) with the tissue lyser MM400 (Retsch, Haan, Germany). After addition of 500 µl Tris-HCl buffer (10 mM, pH 8.5) 10 µl of the resulting suspension was mixed with the Chelex-100 mix (containing 50 µl Tris-HCl buffer (10 mM, pH 8.5), 50 µl Chelex-100 beads (5%; Sigma-Aldrich, Darmstadt, Germany) and 2 µl Proteinase K (20 mg ml^{-1}; Thermo Scientific, Darmstadt, Germany), and incubated (56°C for 45 min, 98°C for 20 min). Marker gene amplification was performed with the repliQa HiFi ToughMix (Quantabio, Beverly, USA) according to the manufacturer's protocol. Marker genes were amplified with the primers MaGo1F, MaGo2F and MaGo3R for the *rbcL* gene and EukA and EukB for the 18S rRNA gene as previously described (Gontcharov *et al.* 2004; Busch & Hess 2022b; Busch *et al.* 2024). The PCR products were subjected to commercial Sanger sequencing (*rbcL* gene of strain SAG 2677: Eurofins Genomics, Ebersberg, Germany, 18S rRNA gene of strains SAG 2677 and ACOI 2703: Microsynth Seqlab, Göttingen, Germany) with the primers MaGo2F, MaGo3R (*rbcL* gene) and EukA, EukB (18S rRNA gene), respectively. The nearly complete gene sequences were assembled from the two overlapping partial reads using the AlignIR™ 2.0 software (LI-COR Biosciences, Lincoln, US) and deposited in GenBank under the accession numbers: PZ567812 (strain SAG 2677, *rbcL* gene), PZ740346 (strain SAG 2677, 18S rRNA gene), PZ740347 (strain ACOI 2703, 18S rRNA gene). The *rbcL* gene sequences were manually added to a comprehensive alignment of Zygnematophyceae with the alignment editor SeaView 4.5.4 (Galtier *et al.* 1996; Gouy *et al.* 2010). A dataset with 93 *rbc*L gene sequences and 1,295 sites was analysed with neighbor joining (NJ), maximum parsimony (MP), and maximum likelihood (ML) methods using the MEGA 11 software (Tamura *et al.* 2021) and RAxML 8.2.6 (Stamatakis 2014). The ML analyses were done with the GTR+I+G model (discrete gamma distribution; five categories), NJ analyses with the p-distance model with the 'pairwise deletion' option, and MP analyses with the subtree-pruning-regrafting (SPR) algorithm. Branch support was assessed by 1,000 bootstrap repetitions for every analysis and added to the ML topology inferred by MEGA 11 shown in the results. A pairwise distance analysis of 11 selected *rbcL* gene sequences was performed with 1,153 sites using MEGA X (Kumar *et al.* 2018). All codon positions were included, but ambiguous positions were removed for each sequence pair (pairwise deletion option). The *rbcL* gene sequence of *Mougeotiopsis calospora* Palla (strain MZCH 580) was excluded from the final phylogenetic analysis as it exhibits relatively low sequence homology with its closest neighbours and leads to distorted topologies in single gene trees (Hess *et al.* 2022).

Results

Morphology, cell cycle and differences of the studied *Mesotaenium* strains

The three investigated strains exhibited elongate cells with subtruncate apices (Fig. 1A–C). The lateral cell walls were either slightly convex (strains SAG 12.97, ACOI 2703) or almost parallel (strain SAG 2677). Cells occurred either single or in chains, the latter of which formed readily in liquid culture as a result of repeated cell division with incomplete cell separation. However, these chains were fragile and easily disrupted by shaking. At the cell apices, a small zone of extracellular mucilage could be present. This mucilage became visible in diluted Indian ink preparations (Fig. 1A, inset) and may contribute to cell-cell adhesion. However, mucilaginous capsules or confluent extracellular polymeric substances, as reported for other saccoderm and placoderm desmids (Kiemle *et al.* 2007; Domozych *et al.* 2014; Busch & Hess 2022a, b) were not observed.

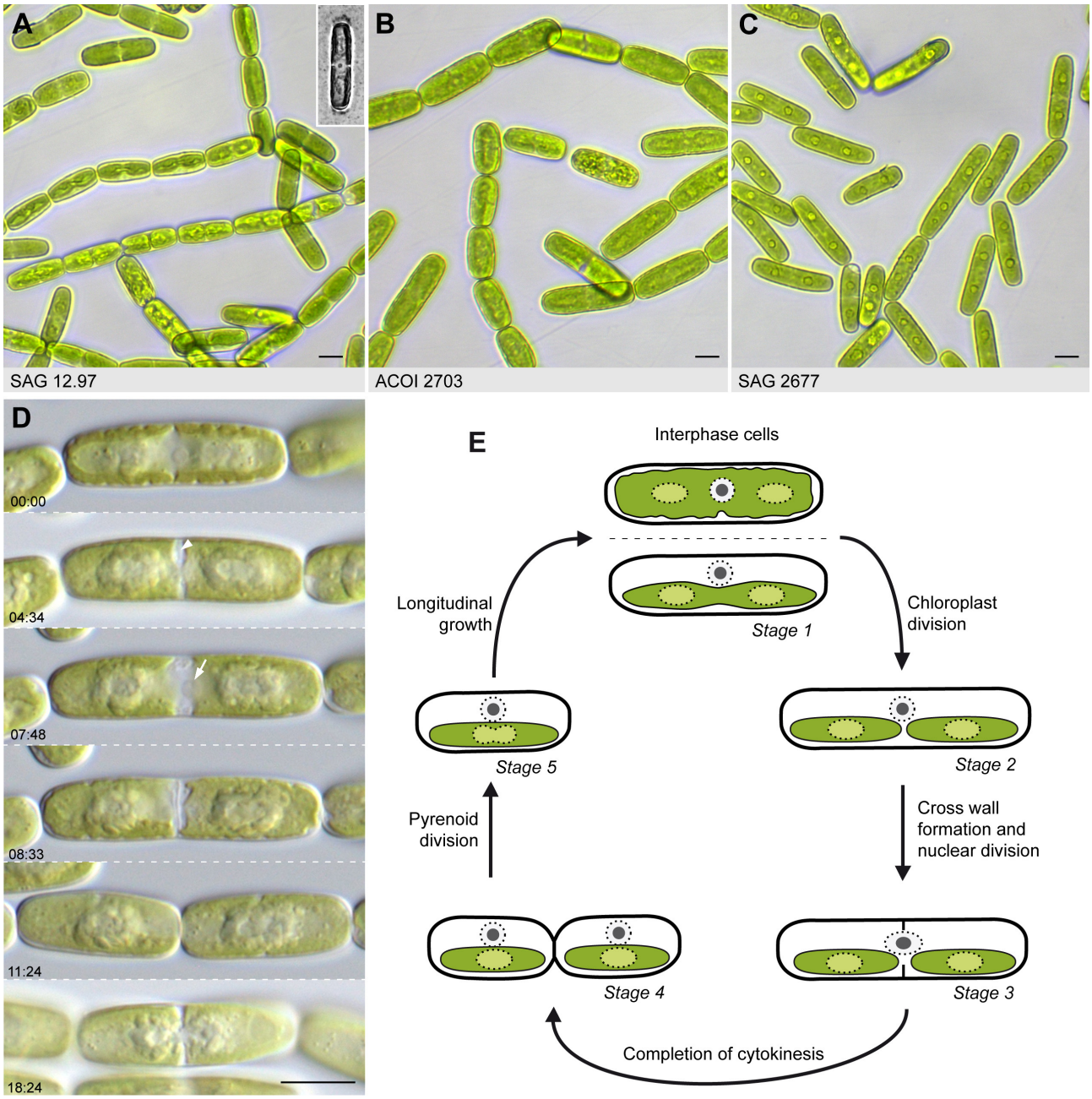

FIGURE 1. General morphology and cell cycle of the studied *Mesotaenium* strains. **A–C** Cell chain formation under axenic culture conditions in strains SAG 12.97 (A), ACOI 2703 (B), and SAG 2677 (C); brightfield. Inset shows sticky apices of strain SAG 12.97 in Indian ink; phase contrast. **D** Time series of cell division in strain SAG 12.97 (time stamps in hh:mm); differential interference contrast. Arrowhead: cross wall, arrow: nucleolus. **E** Schematic of the cell cycle in *Mesotaenium* based on observations of strain SAG 12.97. Scale bars 10 µm.

Time-lapse photography revealed a consistent pattern of cell division particularly with respect to dynamics of chloroplast and pyrenoid division (Fig. 1D, E, Movie S1, S2). Chloroplast division commences relatively early in interphase cells, so that interphase cells harboured either one chloroplast (oftentimes with a central constriction due

to ongoing chloroplast division) or two separate chloroplasts (Fig. 1E, stages 1, 2). Before nuclear division, the cross wall started to form at the cells' mid region. Synthesis of new cell wall material started close to the longitudinal cell wall and moved towards the cells' centre (Fig. 1D, arrowhead; Fig. 1E, stage 3). After nuclear division the two nuclei migrated to opposite parts of the cell and the rest of the cross wall formed and separated the daughter cells (Fig. 1E, stage 4). After completion of cytokinesis, the pyrenoids divided (Fig. 1E, stages 4, 5). During subsequent longitudinal growth of the daughter cells, their chloroplasts expanded. The pyrenoids occupied their typical position in interphase cells, i.e., in the centre of each cell half (Fig. 1E, stage 1). Hence, the three examined strains are characterised by one or two chloroplasts, depending on the cell cycle stage. During interphase, cells typically contained a single chloroplast with a central constriction; shortly after cell division, they possessed a single unconstricted chloroplast, and prior to cytokinesis, two chloroplasts (Figs 2A–I).

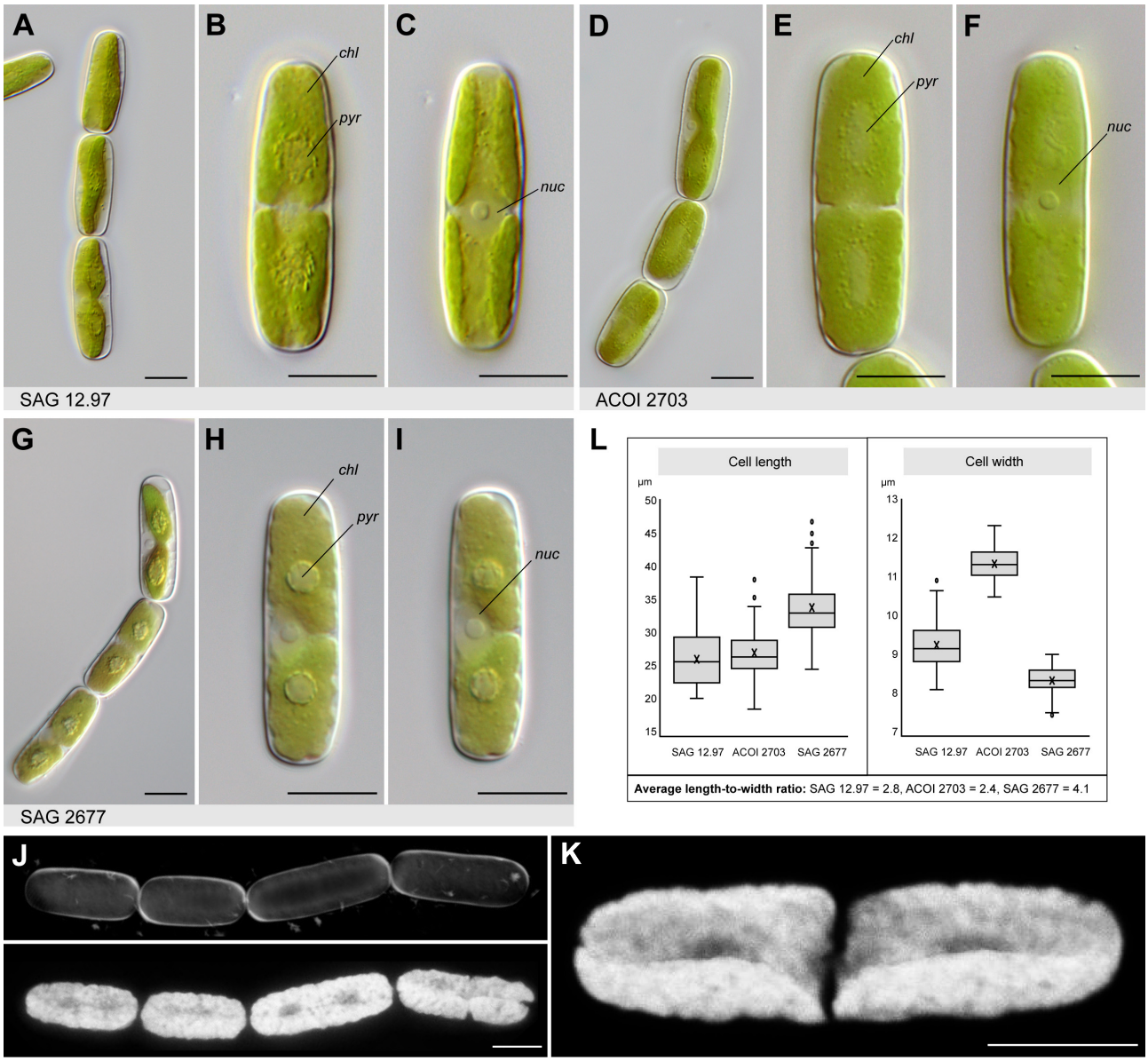

FIGURE 2. Cellular details and cell sizes of the *Mesotaenium* strains. **A–I** Cell chains and single cells in interphase (two focal planes) of strains SAG 12.97 (A–C), ACOI 2703 (D–F), and SAG 2677 (G–I). Note the constricted chloroplasts (*chl*), each with two pyrenoids (*pyr*), and the central nuclei (*nuc*). **J, K** Confocal laser scanning micrographs of strain SAG 12.97. **J** Z-projection of four cells in a chain at different cell cycle stages; Calcofluor White fluorescence (top), chlorophyll autofluorescence (bottom). **K** 3D projection of a cell with two chloroplasts, illustrating the channel-like chloroplast morphology; chlorophyll autofluorescence. **L** Box-and-whisker plots of cell length and cell width (n = 100). Q1, median (Q2), and Q3 correspond to the quartiles below which 25%, 50%, and 75% of the data lie, respectively. The arithmetic mean is indicated by x. Whiskers extend to the most extreme data points within 1.5 × IQR of Q1 and Q3, where IQR = Q3 − Q1. Values beyond these limits are considered outliers and marked as dots. Note the average length-to-width ratios for the strains given below the boxes. Scale bars: 10 µm.

The chloroplasts were plate-like (shortly after cell division, e.g. Fig 2J, first two cells from left) or parietal with folded lateral sides, resulting in a channel-like morphology (in strain SAG 12.97 shortly before cell division) (Fig. 2K). Furthermore, the chloroplast bears undulate margins (Fig. 2B, E, H), which can be missing in cells shortly after cell division. Each cell contained up to two pyrenoids, typically one per cell half. Pyrenoid size and morphology varied among strains (Fig. 2B, E, H). In top view, pyrenoids were circular or slightly elliptic in strain SAG 12.97 (Figs 2B), elliptic to elongate in strain ACOI 2703 (Fig. 2E), and circular in strain SAG 2677 (Fig. 2H). Pyrenoids were readily visible in strains SAG 12.97 and SAG 2677 due to surrounding starch grains (Fig. 2B, H), whereas those of strain ACOI 2703 were indistinct (Fig. 2E). In all strains, the nucleus was situated either close to the chloroplast constriction or between two chloroplasts (Figs 2C, F, I). It was usually displaced towards the lateral cell wall, thus not exactly in the longitudinal cell axis. Interphase nuclei ranged in size from 6 µm (strains SAG 12.97 and SAG 2677) to 7 µm (strain ACOI 2703) and contained a prominent central nucleolus. Apart from pyrenoid morphology, the studied strains differed markedly in cell dimensions, particularly in cell width and in the average length-to-width ratio (Fig. 2L).

Phylogenetic position and genetic differences of the *Mesotaenium* strains

We inferred molecular phylogenies of the *rbcL* gene with the three studied strains in a comprehensive phylogenetic context of other zygnematophytes (93 sequences). The best ML-based phylogenetic tree largely agrees with previous phylogenies (Busch & Hess 2022a; Hess *et al.* 2022) and recovered the orders Desmidiales, Spirogyrales, and Serritaeniales (Fig. S1, S2). All three investigated strains branch with *Serritaenia* species and saccoderm desmids of lineage Meso-1 (nomenclature according to Busch & Hess 2022a with strong statistical support (Fig. 3)), confirming their placement within the order Serritaeniales. In ML analyses conducted with the MEGA 11 software, the three investigated strains formed the deepest branching clade in Serritaeniales (support 99/52/99). In contrast, analyses with RAxML suggested that Meso-1 was the deepest-branching lineage, highlighting the need of multigene phylogenies to achieve more robust resolution of the deeper branches. The branching pattern among the three studied strains (Fig. 3) lacked statistical support and varied depending on the phylogenetic method and software (MEGA vs. RAxML). However, the three lineages on genus level, i.e., *Mesotaenium*, *Serritaenia* and Meso-1, were clearly distinct and well-supported. Cross-lineage genetic differences in the *rbcL* gene ranged from 19–23 %, whereas the three studied strains showed genetic differences of about 7 %, comparable to values inside other zygnematophycean genera such as *Serritaenia* (Fig. 3). Genetic differences in the 18S rRNA gene of the three studied strains were between 0.1–0.3 % (corresponding to 2–6 nucleotides), illustrating that the 18S rRNA gene is too conserved to differentiate zygnematophytes on the species level.

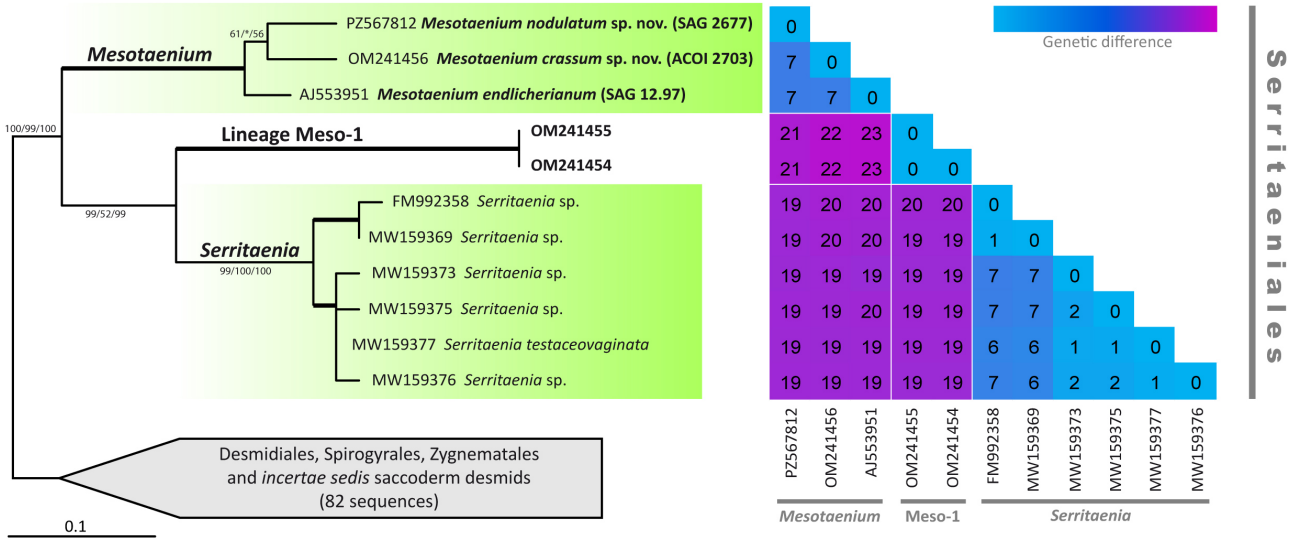

FIGURE 3. Molecular phylogeny of the genus *Mesotaenium* and genetic differences of analysed taxa. The tree represents an unrooted ML phylogeny of 93 zygnematophycean *rbcL* gene sequences with support values > 50 % shown on the respective branches (ML/MP/NJ). Branches with maximum support (100/100/100) are bold. Scale bar = 0.1 nucleotide substitutions per site. The table on the right displays the percent genetic distances of the shown taxa inferred by pairwise comparisons of *rbcL* gene sequences.

Discussion

The *rbcL* gene-based phylogeny and detailed morphological data support a close relationship of strains SAG 12.97, ACOI 2703 and SAG 2677, and their affiliation to the Serritaeniales (Hess *et al.* 2022). The observed *rbcL* sequence divergence of about 7% among the three strains agrees well with values typically reported for interspecific genetic differences in other algal and embryophyte genera (Chase *et al.* 2005; Newmaster *et al.* 2006; Hall *et al.* 2010). Moreover, the strains display clear morphological differences, especially in cell size, pyrenoid structure, and the morphology of starch granules. Taken together, the results support the delineation of the three strains as distinct species, which require formal taxonomic designations.

A particularly complex case concerns strain SAG 12.97 and its assignment to *M. endlicherianum*, the type species of the genus *Mesotaenium*. Historically, strain SAG 12.97 was identified as *M. endlicherianum* by the collector in 1991 and has been consistently referred to this name in the subsequent literature, despite notes questioning its identity (Gontcharov *et al.* 2003, 2004; Hall *et al.* 2008). Furthermore, several experimental studies and molecular datasets, applied the name *M. endlicherianum*, and did not question or reevaluate the taxonomic identity of strain SAG 12.97 (Cheng *et al.* 2019; Carrillo-Carrasco *et al.* 2023; Dadras *et al.* 2023a; Rieseberg *et al.* 2023). A name change at this point would generate significant confusion, similar to the problems encountered with other intensely studied organisms of the genera *Physcomitrium* (Bridel) Bridel (1827: 793, 815) */Physcomitrella* Bruch & Schimper (1849: 13) (Bridel-Brideri 1827; Schimper *et al.* 1836; Medina *et al.* 2019), *Ulva* Linnaeus (1753:1163)/*Enteromorpha* Link (1820: 5) (Linnaeus 1753; Link 1820; Hayden *et al.* 2003), and *Scenedesmus* Meyen (1829: 774)/*Desmodesmus* (Chodat) S.S. An, T. Friedl & E. Hegewald (1999: 427) (Meyen 1829; An *et al.* 1999; Hegewald *et al.* 2010).

In fact, strain SAG 12.97 does not correspond in every detail to the original description of *M. endlicherianum* (Nägeli 1849), namely the elliptic pyrenoids (circular in orig. fig.), the division of pyrenoids (*de novo* formation in orig. descr.), undulating chloroplast edges (not reported in orig. descr.), and the subtruncate cell apices (rounded in orig. fig.) (compare Fig. 4A and B). However, notable similarities exist as well, namely the general cell proportions (strain SAG 12.97: 20–38 × 8–11 µm, length-to-width ratio: 2–4; *M. endlicherianum*: 32–45 × 9–11 µm, length-to-width ratio: 3–4) and the presence of one or two chloroplasts and pyrenoids. While Nägeli presumably examined material collected from natural populations, our morphological observations are based on cultured material. Like many other species, saccoderm desmids exhibit variation in certain morphological features in response to environmental conditions such as nutrient and water availability as well as light intensity (Busch & Hess 2022b; Dadras *et al.* 2023a; Rieseberg *et al.* 2023; Busch *et al.* 2024). In particular, the appearance of chloroplasts and pyrenoids may differ between cultured cells and cells observed in natural populations. In *Serritaenia*, for example, the chloroplasts of cultured cells often exhibit larger sizes and more complex morphologies than those observed in nature (Busch & Hess 2022b)—a phenomenon also observed in other lineages of yet uncharacterized saccoderm desmids (unpublished observations). Furthermore, Nägeli stated that he had never observed nuclei, suggesting that some intracellular structures may have been difficult to resolve with the optical equipment available at the time (Nägeli 1849). These differences may account for some of the discrepancies observed in chloroplast shape as well as pyrenoid morphology and formation. However, other important characters such as cell size, number of chloroplasts, and number of pyrenoids are unlikely to be affected by the technical limitations mentioned. Most importantly, previous studies of *Serritaenia* and *Cylindrocystis* have shown that especially the cell width is a relatively stable character of genetically distinct strains and, hence, valuable for species delimitation (Barcytė *et al.* 2020; Busch & Hess 2022b). It should also be noted that none of the 50 *Mesotaenium*-like strains collected by the authors of this study better fit the original description of *M. endlicherianum* by Nägeli, and that relocating the exact sampling site of this species in the Zurich area was not feasible.

We therefore epitypify *M. endlicherianum* based on strain SAG 12.97, despite the minor morphological conflicts mentioned above. This will provide nomenclatural stability, continuity with existing literature, and a clear reference point for future taxonomic revisions of *Mesotaenium*-like zygnematophytes. In case of the other two strains ACOI 2703 and SAG 2677, no original species description matches the strains' morphology. Hence, we describe two new species, namely *M. crassum sp. nov.* for ACOI 2703 and *M. nodulatum sp. nov.* for strain SAG 2677. The latter strain resembles *Mesotaenium truncatum* West & G.S. West (1904: 54) (West & West 1904) to some extent (Fig. 4), including the cylindrical cell shape, the truncate apices, the axile chloroplasts with a notch visible shortly before division, and one to two pyrenoids (West & West 1904). However, the cell width does not match (strain SAG 2677: 7–9 µm; *M. truncatum*: 9.5–10 µm) so that we refrain from applying this name to strain SAG 2677. The nomenclatural acts and associated information follow in the taxonomy section.

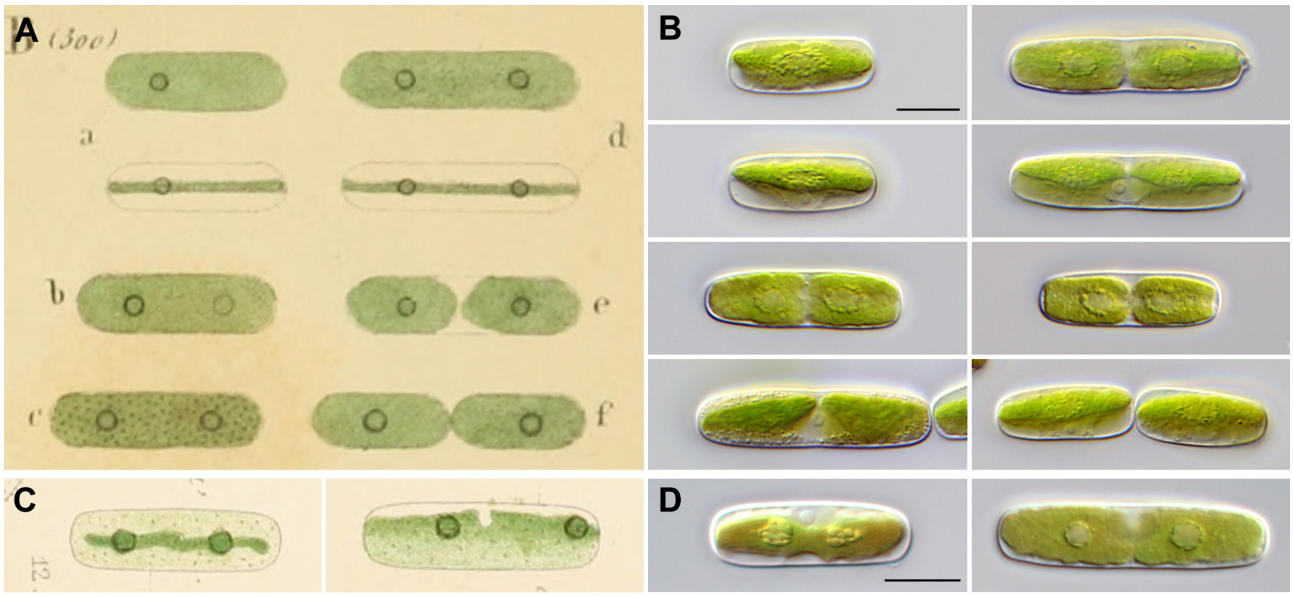

FIGURE 4. Comparison of original illustrations of *M. endlicherianum* and *M. truncatum* and corresponding cell cycle stages of the studied strains. A Original figure of *M. endlicherianum* (Plate VI B, Nägeli 1849)). B Cells of strain SAG 12.97 at corresponding cell cycle stages to A. C Original figure of *M. truncatum* (Plate V fig. 12, (West & West 1904). D Cells of strain SAG 2677 at corresponding cell cycle stages to C. Scale bars: 10 µm.

The taxonomic evaluation combined with molecular phylogenetic data, now allow a robust assignment of the genus *Mesotaenium* in the phylogenetic tree of zygnematophytes, namely to lineage Meso-2 (Busch & Hess 2022a). The morphological analyses further reveal a set of valuable and consistent phenotypic traits for *Mesotaenium* as defined here. These include unicells with subtruncate apices, a length-to-width ratio of 2–6, one to two chloroplasts with undulating margins (depending on environmental conditions), and the frequent formation of cell chains. This combination of morphological characters differs from those found in the closely related lineages Meso-1 and *Serritaenia* (Busch & Hess 2022a), hence supporting the recognition of *Mesotaenium* as a distinct genus. Furthermore, none of the other currently known "*Mesotaenium*" strains group with the lineage comprising *Mesotaenium endlicherianum* and thus require a separate taxonomic reassessment.

Taxonomy

Class **Zygnematophyceae** Round ex Guiry 2013

Genus ***Mesotaenium*** Nägeli 1849: 108

Emended description: Elongate unicells (length-to-width ratio of 2–6) with subtruncate apices; one to two chloroplasts per cell, with undulating margins depending on environmental conditions, plate-like or parietal with folded lateral sides; one to two pyrenoids (lentiform or circular), pyrenoid division after cell division; nucleus vesicular with central nucleolus, displaced by the chloroplast towards the cell wall; frequent formation of cell chains.

Type species: *Mesotaenium endlicherianum* Nägeli 1849: 108

Mesotaenium endlicherianum Nägeli 1849: 108

Emended description: Cells elongate (20–38 µm long, 8–11 µm wide) with subtruncate apices; one to two chloroplasts per cell, in culture often with undulating margins and channel-like morphology (parietal); one to two lentiform pyrenoids (4.5–7 × 2–3 µm); nucleus vesicular with central nucleolus, displaced by the chloroplast towards the cell wall. Cytoplasm colourless, sometimes containing globular inclusions. In undisturbed culture, cells readily form fragile chains by incomplete separation after cell division. No zygospores observed.

Lectotype (designated here): Illustration in Nägeli 1849: Plate VI B.

Epitype (designated here): The authentic strain SAG 12.97 is permanently cryopreserved in a metabolically inactive state (cryopreserved in liquid nitrogen) in the SAG, University of Göttingen, Germany, under the accession number Z002077809 (cryopreserved batches also stored under Z002077810-Z002077813). Strain origin: plankton, Quiaios, Lagoa das Braças, Portugal; collected 1991, leg. O. Lourenço.

Epitype generating strain: SAG 12.97

PhycoBank ID (of lectotype and epitype): http://phycobank.org/107833

Reference sequence: AJ553951 (*rbcL* gene sequence of strain SAG 12.97), GCA_009602735 (genome of strain SAG 12.97)

Note: Type species of the genus *Mesotaenium* Nägeli 1849

Mesotaenium crassum *sp. nov.*

Description: Cells elongate (18–38 µm long, 10–12 µm wide) with subtruncate apices; one to two chloroplasts per cell, in culture often with undulating margins; one to two lentiform pyrenoids (5.5–8 × 2.5–4.5 µm), difficult to discern; nucleus vesicular with central nucleolus, displaced by the chloroplast towards the cell wall. In undisturbed culture, cells readily form fragile chains by incomplete separation after cell division. No zygospores observed.

Diagnosis: Differs from *M. endlicherianum* and *M. nodulatum* by its faintly visible pyrenoids and a lower length-to-width ratio.

Etymology: *crassus, -a, -um* [Latin] = thick. The epithet refers to the relatively low length-to-width ratio, which gives the cells a thick appearance.

Holotype (designated here): The authentic strain ACOI 2703 is permanently cryopreserved in a metabolically inactive state (cryopreserved in liquid nitrogen) in the SAG, University of Göttingen, Germany, under the accession number Z002077814 (cryopreserved batches also stored under Z002077815– Z002077818). Strain origin: brook, between Ceada and Miranda do Douro, Spain; collected 2006, leg. L. Santos.

Type generating strain: ACOI 2703

PhycoBank ID: http://phycobank.org/107829

Reference sequence: OM241456 (*rbcL* gene sequence of strain ACOI 2703).

Mesotaenium nodulatum *sp. nov.*

Description: Cells elongate (24–47 µm long, 7–9 µm wide) with subtruncate apices; one to two chloroplasts per cell, in culture often with undulating margins; one to two nearly circular pyrenoids (3.6–4.7 × 3.5–4.2 µm); nucleus vesicular with central nucleolus, displaced by the chloroplast towards the cell wall. In undisturbed culture, cells readily form fragile chains by incomplete separation after cell division. No zygospores observed.

Diagnosis: Differs from *M. endlicherianum* and *M. crassum* by its circular pyrenoids.

Etymology: *nodulatus, -a, -um* [Latin] = provided with nodules/small knobs. The epithet refers to the knob-like appearance of the pyrenoids.

Holotype (designated here): The authentic strain SAG 2677 is permanently cryopreserved in a metabolically inactive state (cryopreserved in liquid nitrogen) in the SAG, University of Göttingen, Germany, under the accession number Z002077819 (cryopreserved batches also stored under Z002077820 – Z002077823). Strain origin: forest trail, Gemünd-Malsbenden, Germany; collected 2020, leg. K.H. Linne von Berg.

Type generating strain: SAG 2677

PhycoBank ID: http://phycobank.org/107830

Reference sequence: PZ567812 (*rbcL* gene sequence of strain SAG 2677).

Acknowledgements

We thank the curators of the Culture Collection of Algae at Göttingen University (SAG) and the Coimbra Culture Collection of Algae (ACOI) for providing algal cultures, and Helen Kamp for providing 18S rRNA sequences of the studied strains. This work was supported by the German Research Foundation, projects 417585753 and 491244984 to SH.

References

An, S.S., Friedl, T. & Hegewald, E. (1999) Phylogenetic Relationships of *Scenedesmus* and *Scenedesmus*- like Coccoid Green Algae as Inferred from ITS-2 rDNA Sequence Comparisons. *Plant Biology* 1: 418–428. https://doi.org/10.1111/j.1438-8677.1999.tb00724.x

Barcytė, D., Pilátová, J., Mojzeš, P. & Nedbalová, L. (2020) The arctic *Cylindrocystis* (Zygnematophyceae, Streptophyta) green algae are genetically and morphologically diverse and exhibit effective accumulation of polyphosphate. *Journal of Phycology* 56: 217–232. https://doi.org/10.1111/jpy.12931

de Bary, A. (1858) *Untersuchungen über die Familie der Conjugaten (Zygnemeen und Desmidieen): Ein Beitrag zur physiologischen und beschreibenden Botanik*. Förstnersche Buchhandlung, Leipzig, 82 pp., pl. I–VIII. https://doi.org/10.5962/bhl.title.63789

Berggren, S. (1871) *Bidrag till kännedom om fanerogamfloran vid Diskobugten och Auleitsivik-fjorden på Grönlands vestkust*. *Öfversigt af Förhandlingar Kongl. Vetenskaps-akademiens*: 853–897.

Bridel-Brideri, S.E. (1827) *Bryologia Universa seu Systematica ad Novam Methodum Dispositio, Historia et Descriptio omnium Muscorum Frondosorum Hucusque Cognitorum cum Synonymia ex Auctoribus Probatissimis. II*. Sumtibus Joan. Ambros. Barth, Lepzig, 848 pp., pl. I–X, Suppl. I–Suppl. III. https://doi.org/10.5962/bhl.title.60260

Buech, G. (1967) Zur Taxonomie und Cytologie der Gattung *Mesotaenium* Nägeli. Dissertation. Universität des Saarlandes.

Busch, A. & Hess, S. (2022a) A diverse group of underappreciated zygnematophytes deserves in-depth exploration. *Applied Phycology*: 1–18. https://doi.org/10.1080/26388081.2022.2081819

Busch, A. & Hess, S. (2022b) Sunscreen mucilage: a photoprotective adaptation found in terrestrial green algae (Zygnematophyceae). *European Journal of Phycology* 57: 107–124. https://doi.org/10.1080/09670262.2021.1898677

Busch, A., Slominski, E., Remias, D., Procházková, L. & Hess, S. (2024) A mesophilic relative of common glacier algae, *Ancylonema palustre* sp. nov., provides insights into the induction of vacuolar pigments in zygnematophytes. *Environmental Microbiology* 26: e16680. https://doi.org/10.1111/1462-2920.16680

Carrillo-Carrasco, V.P., Hernández-García, J. & Weijers, D. (2023) Electroporation-based delivery of proteins in *Penium margaritaceum* and other zygnematophycean algae. *Physiologia Plantarum* 175: e14121. https://doi.org/10.1111/ppl.14121

Chase, M.W., Salamin, N., Wilkinson, M., Dunwell, J.M., Kesanakurthi, R.P., Haidar, N. & Savolainen, V. (2005) Land plants and DNA barcodes: short-term and long-term goals. *Philosophical Transactions of the Royal Society B: Biological Sciences* 360: 1889–1895. https://doi.org/10.1098/rstb.2005.1720

Cheng, S., Xian, W., Fu, Y., Marin, B., Keller, J., Wu, T., Sun, W., Li, X., Xu, Y. & Zhang, Y. (2019) Genomes of subaerial Zygnematophyceae provide insights into land plant evolution. *Cell* 179: 1057–1067. https://doi.org/10.1016/j.cell.2019.10.019

Civáň, P., Foster, P.G., Embley, M.T., Séneca, A. & Cox, C.J. (2014) Analyses of Charophyte Chloroplast Genomes Help Characterize the Ancestral Chloroplast Genome of Land Plants. *Genome Biology and Evolution* 6: 897–911. https://doi.org/10.1093/gbe/evu061

Cushman, J.A. (1906) New England Desmids of the Sub-Family Saccodermae. *Bulletin of the Torrey Botanical Club* 33: 343. https://doi.org/10.2307/2478911

Dadras, A., Fürst-Jansen, J.M.R., Darienko, T., Krone, D., Scholz, P., Sun, S., Herrfurth, C., Rieseberg, T.P., Irisarri, I., Steinkamp, R., Hansen, M., Buschmann, H., Valerius, O., Braus, G.H., Hoecker, U., Feussner, I., Mutwil, M., Ischebeck, T., de Vries, S., Lorenz, M. & de Vries, J. (2023a) Environmental gradients reveal stress hubs pre-dating plant terrestrialization. *Nature Plants* 9: 1419–1438. https://doi.org/10.1038/s41477-023-01491-0

Dadras, A., Rieseberg, T.P., Zegers, J.M.S., Fürst-Jansen, J.M.R., Irisarri, I., de Vries, J. & de Vries, S. (2023b) Accessible versatility underpins the deep evolution of plant specialized metabolism. *Phytochemistry Reviews*. https://doi.org/10.1007/s11101-023-09863-2

De Araújo, C.B., De Mattos Bicudo, C.E., Da Silva, T.G., Šťastný, J., Trumhová, K. & Škaloud, P. (2022) Hidden generic diversity in desmids: description of *Pseudomicrasterias* gen. nov. (Desmidiaceae, Zygnematophyceae). *Phycologia* 61: 227–240. https://doi.org/10.1080/00318884.2022.2031781

Domozych, D.S., Sørensen, I., Popper, Z.A., Ochs, J., Andreas, A., Fangel, J.U., Pielach, A., Sacks, C., Brechka, H. & Ruisi-Besares, P.

(2014) Pectin metabolism and assembly in the cell wall of the charophyte green alga *Penium margaritaceum*. *Plant Physiology* 165: 105–118.
https://doi.org/10.1104/pp.114.236257

Fujimoto, M., Shimizu, Y., Ito, Y., Ebine, K., Minamino, N., Kanazawa, T., Fukao, Y., Nakano, A., Uemura, T. & Ueda, T. (2025) Neofunctionalization of VAMP7 opened up a plant-unique vacuolar transport pathway. *Current Biology* 35: 2630–2641.e10.
https://doi.org/10.1016/j.cub.2025.04.062

Galtier, N., Gouy, M. & Gautier, C. (1996) SEAVIEW and PHYLO_WIN: two graphic tools for sequence alignment and molecular phylogeny. *Bioinformatics* 12: 543–548.
https://doi.org/10.1093/bioinformatics/12.6.543

Gontcharov, A.A. (2008) Phylogeny and classification of Zygnematophyceae (Streptophyta): current state of affairs. *Fottea* 8: 87–104.
https://doi.org/10.5507/fot.2008.004

Gontcharov, A.A., Marin, B. & Melkonian, M. (2003) Molecular phylogeny of conjugating green algae (Zygnemophyceae, Streptophyta) inferred from SSU rDNA sequence comparisons. *Journal of Molecular Evolution* 56: 89–104.
https://doi.org/10.1007/s00239-002-2383-4

Gontcharov, A.A., Marin, B. & Melkonian, M. (2004) Are combined analyses better than single gene phylogenies? A case study using SSU rDNA and rbc L sequence comparisons in the Zygnematophyceae (Streptophyta). *Molecular Biology and Evolution* 21: 612–624.
https://doi.org/10.1093/molbev/msh052

Gontcharov, A.A. & Melkonian, M. (2010) Molecular Phylogeny and Revision of the Genus *Netrium* (Zygnematophyceae, Streptophyta): *Nucleotaenium* gen. nov. *Journal of Phycology* 46: 346–362.
https://doi.org/10.1111/j.1529-8817.2010.00814.x

Gouy, M., Guindon, S. & Gascuel, O. (2010) SeaView version 4: a multiplatform graphical user interface for sequence alignment and phylogenetic tree building. *Molecular Biology and Evolution* 27: 221–224.
https://doi.org/10.1093/molbev/msp259

Guiry, M.D. & Guiry, G.M. (2026) AlgaeBase. World-wide electronic publication. Available from: https://www.algaebase.org (accessed 30 July 2026)

Hall, J.D., Fučíková, K., Lewis, L.A. & Karol, K.G. (2010) An assessment of proposed DNA barcodes in freshwater green algae. *Cryptogam Algol* 31: 529–55.

Hall, J.D., Karol, K.G., McCourt, R.M. & Delwiche, C.F. (2008) Phylogeny of the Conjugating Green Algae Based on Chloroplast and Mitochondrial Nucleotide Sequence Data. *Journal of Phycology* 44: 467–477.
https://doi.org/10.1111/j.1529-8817.2008.00485.x

Hall, J.D. & McCourt, R. (2016) Zygnematophyta. *In*: *Handbook of the protists*. pp. 135–163.
https://doi.org/10.1007/978-3-319-32669-6_41-1

Hansgirg, A. (1886) *Prodromus der Algenflora von Böhmen Erster Theil. Enthaltend die Rhodophyceen, Phaeophyceen und einen Teil der Chlorophyceen*. Řivnáč, Prag, 286 pp.

Hayden, H.S., Blomster, J., Maggs, C.A., Silva, P.C., Stanhope, M.J. & Waaland, J.R. (2003) Linnaeus was right all along: *Ulva* and *Enteromorpha* are not distinct genera. *European Journal of Phycology* 38: 277–294.
https://doi.org/10.1080/1364253031000136321

Hegewald, E., Wolf, M., Keller, A., Friedl, T. & Krienitz, L. (2010) ITS2 sequence-structure phylogeny in the Scenedesmaceae with special reference to *Coelastrum* (Chlorophyta, Chlorophyceae), including the new genera *Comasiella* and *Pectinodesmus*. *Phycologia* 49: 325–335.
https://doi.org/10.2216/09-61.1

Hess, S., Williams, S.K., Busch, A., Irisarri, I., Delwiche, C.F., De Vries, S., Darienko, T., Roger, A.J., Archibald, J.M., Buschmann, H., Von Schwartzenberg, K. & De Vries, J. (2022) A phylogenomically informed five-order system for the closest relatives of land plants. *Current Biology* 32: 4473–4482.e7.
https://doi.org/10.1016/j.cub.2022.08.022

Kiemle, S.N., Domozych, D.S. & Gretz, M.R. (2007) The extracellular polymeric substances of desmids (Conjugatophyceae, Streptophyta): chemistry, structural analyses and implications in wetland biofilms. *Phycologia* 46: 617–627.
https://doi.org/10.2216/06-97.1

Kumar, S., Stecher, G., Li, M., Knyaz, C. & Tamura, K. (2018) MEGA X: molecular evolutionary genetics analysis across computing platforms. *Molecular Biology and Evolution* 35: 1547–1549.
https://doi.org/10.1093/molbev/msy096

Lagerheim, G. (1886) Algologiska Bidrag. I. Contributions algologique à la flore de la Suède. *Botaniska Notiser*: 44–50.

Link, H.F. (1820) *Epistola Ad Virum Celeberrimum Nees Ab Esenbeck De Algis Aquaticis In Genera Disponendis*. Sumtibus Adolphi Marcus, Bonn, 8 pp., pl. I.

Linnaeus (1753) *Species Plantarum: Exhibentes Plantas Rite Cognitas, Ad Genera Relatas, Cum Differentiis Specificis, Nominibus Trivialibus, Synonymis Selectis, Locis Natalibus, Secundum Systema Sexuale Digestas. II*. Impensis Laurentii Salvii, Stockholm, 640 pp.
https://doi.org/10.5962/bhl.title.59734

Luo, J. & Hall, B.D. (2007) A Multistep Process Gave Rise to RNA Polymerase IV of Land Plants. *Journal of Molecular Evolution* 64: 101–112.
https://doi.org/10.1007/s00239-006-0093-z

Marks, J. & Petersen, M. (2026) Early occurrence of caffeoylshikimic acid esterase (CSE) activity in the hornwort *Anthoceros agrestis*. *Planta* 263: 49.
https://doi.org/10.1007/s00425-025-04915-7

Matasci, N., Hung, L.-H., Yan, Z., Carpenter, E.J., Wickett, N.J., Mirarab, S., Nguyen, N., Warnow, T., Ayyampalayam, S. & Barker, M. (2014) Data access for the 1,000 Plants (1KP) project. *Gigascience* 3: 2047–217X.
https://doi.org/10.1186/2047-217x-3-17

McFadden, G.I. & Melkonian, M. (1986) Use of Hepes buffer for microalgal culture media and fixation for electron microscopy. *Phycologia* 25: 551–557.
https://doi.org/10.2216/i0031-8884-25-4-551.1

Medina, R., Johnson, M.G., Liu, Y., Wickett, N.J., Shaw, A.J. & Goffinet, B. (2019) Phylogenomic delineation of *Physcomitrium* (Bryophyta: Funariaceae) based on targeted sequencing of nuclear exons and their flanking regions rejects the retention of *Physcomitrella*, *Physcomitridium* and *Aphanorrhegma*. *Journal of Systematics and Evolution* 57: 404–417.
https://doi.org/10.1111/jse.12516

Meyen, F.J.F. (1829) Beobachtungen über einige niedere Algenformen. *Nova Acta Physico-Medica* 14: 768–778.

Nägeli, C. (1849) *Gattungen einzelliger Algen: physiologisch und systematisch bearbeitet*. Friedrich Schulthess, Zürich, 138 pp., pl. I–VIII.
https://doi.org/10.5962/bhl.title.6805

Newmaster, S.G., Fazekas, A.J. & Ragupathy, S. (2006) DNA barcoding in land plants: evaluation of rbcL in a multigene tiered approach. *Botany* 84: 335–341.
https://doi.org/10.1139/b06-047

Procházková, L., Řezanka, T., Nedbalová, L. & Remias, D. (2021) Unicellular versus Filamentous: The Glacial Alga *Ancylonema alaskana* comb. et stat. nov. and Its Ecophysiological Relatedness to *Ancylonema nordenskioeldii* (Zygnematophyceae, Streptophyta). *Microorganisms* 9: 1103.
https://doi.org/10.3390/microorganisms9051103

Ralfs, J. (1848) *The British Desmidieae: The Drawings by Edw. Jenner*. Reeve, London, 226 pp., pl. I–XXXV.

Rieseberg, T.P., Dadras, A., Bergschmidt, L.I.N., Bierenbroodspot, M.J., Fürst-Jansen, J.M.R., Irisarri, I., de Vries, S., Darienko, T. & de Vries, J. (2023) Divergent responses in desiccation experiments in two ecophysiologically different Zygnematophyceae. *Physiologia Plantarum* 175: e14056.
https://doi.org/10.1111/ppl.14056

Rieseberg, T.P., Dadras, A., Darienko, T., Post, S., Herrfurth, C., Fürst-Jansen, J.M.R., Hohnhorst, N., Petroll, R., Rensing, S.A., Pröschold, T., De Vries, S., Irisarri, I., Feussner, I. & De Vries, J. (2025) Time-resolved oxidative signal convergence across the algae–embryophyte divide. *Nature Communications* 16: 1780.
https://doi.org/10.1038/s41467-025-56939-y

de Roij, M., Hernández García, J., Das, S., Borst, J.W. & Weijers, D. (2025) ARF degradation defines a deeply conserved step in auxin response. *Nature Plants* 11: 717–724.
https://doi.org/10.1038/s41477-025-01975-1

Schimper, W.-P., Bruch, P., Gümbel, T. & Schimper, W.-P. (1836) *Bryologia Europae, seu Genera Muscorum Europaeorum Monographice Illustrata. III*. Sumptibus Librariae E. Schweizerbart, Stuttgart, 305 pp., pl. 1–305.
https://doi.org/10.5962/bhl.title.50508

Schindelin, J., Arganda-Carreras, I., Frise, E., Kaynig, V., Longair, M., Pietzsch, T., Preibisch, S., Rueden, C., Saalfeld, S. & Schmid, B. (2012) Fiji: an open-source platform for biological-image analysis. *Nature Methods* 9: 676–682.
https://doi.org/10.1038/nmeth.2019

Stamatakis, A. (2014) RAxML version 8: a tool for phylogenetic analysis and post-analysis of large phylogenies. *Bioinformatics* 30: 1312–1313.
https://doi.org/10.1093/bioinformatics/btu033

Tamura, K., Stecher, G. & Kumar, S. (2021) MEGA11: Molecular Evolutionary Genetics Analysis Version 11. *Molecular Biology and Evolution* 38: 3022–3027.

https://doi.org/10.1093/molbev/msab120
Teiling, E. (1954) *Actinotaenium*, genus *Desmidiacearum resuscitatum*. *Botanisk Notiser* 4: 376–426.
West, W. & West, G.S. (1904) *A monograph of the British Desmidiaceae. I*. The Ray Society, London, 224 pp., pl. 1–32.
https://doi.org/10.5962/bhl.title.1619

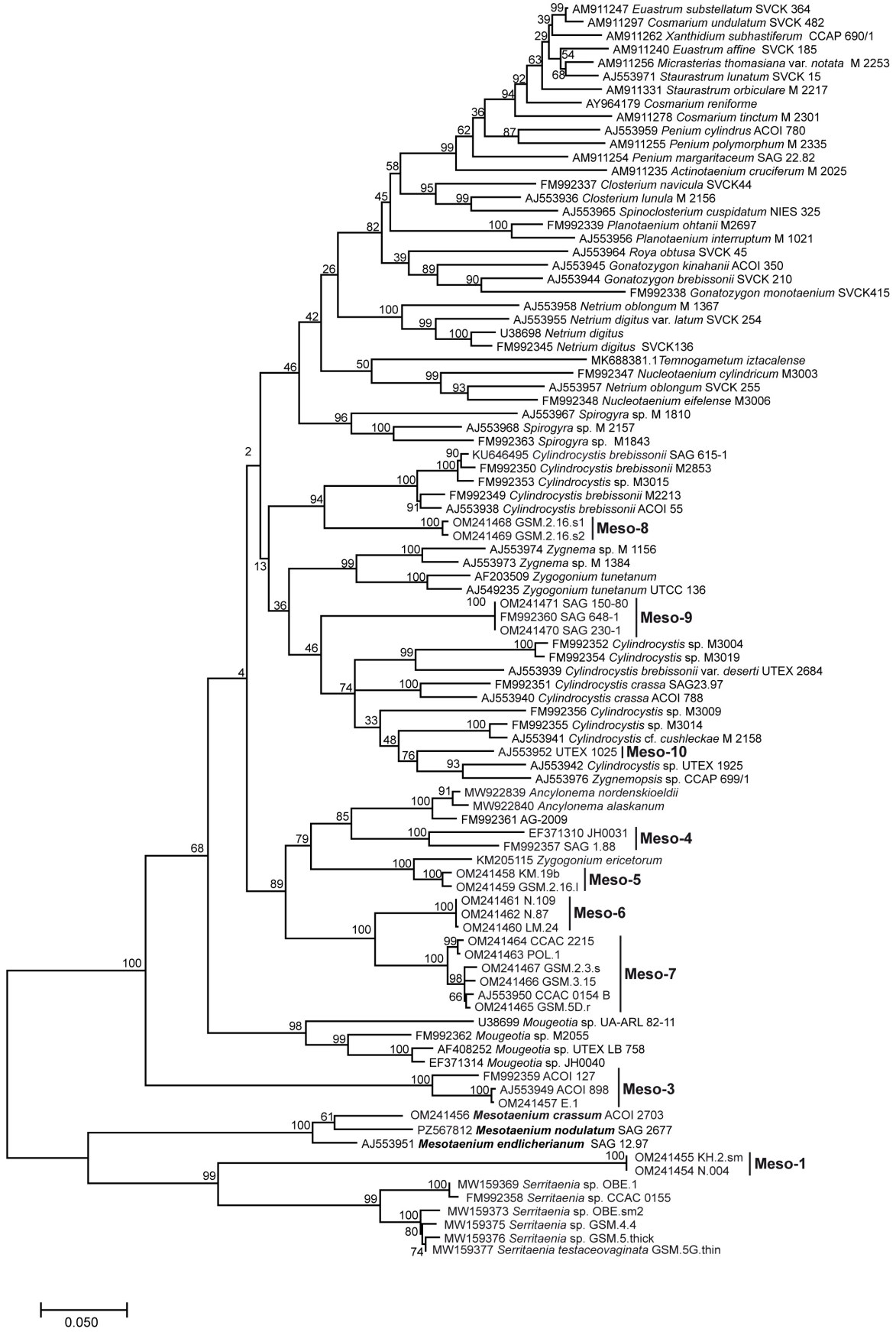

FIGURE S1. Unrooted ML phylogeny of 93 zygnematophycean *rbcL* gene sequences inferred with the software MEGA 11 (Tamura *et al.* 2021). Values at the branches denote bootstrap support (percent) of 1,000 replicates. Scale bar = 0.05 nucleotide substitutions per site.

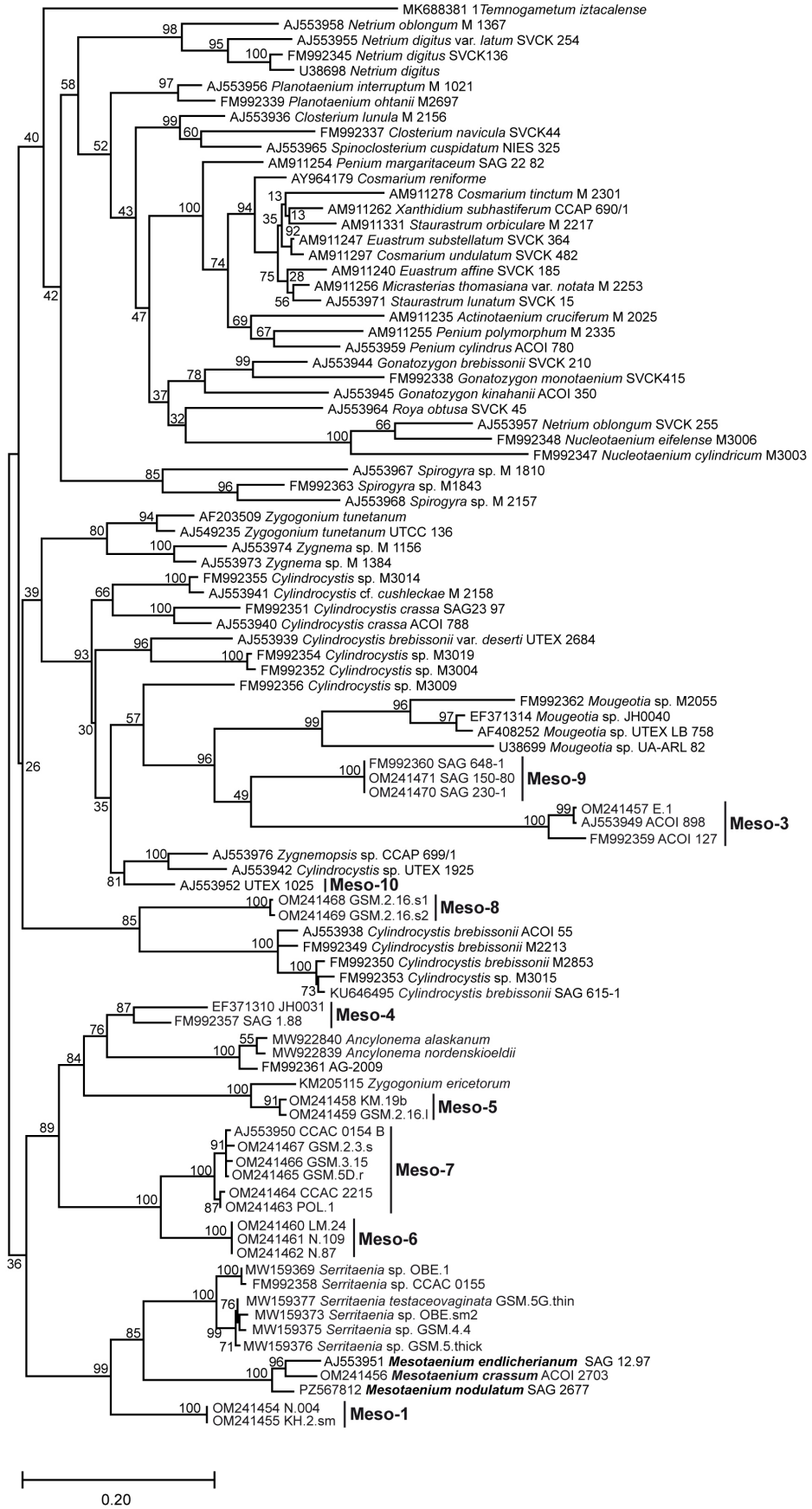

FIGURE S2. Unrooted ML phylogeny of 93 zygnematophycean *rbcL* gene sequences inferred with the software RAxML 8.2.6 (Stamatakis 2014). Values at the branches denote bootstrap support (percent) of 1,000 replicates. Scale bar = 0.2 nucleotide substitutions per site.